Materials Science & Engineering A 728 (2018) 40–44

Contents lists available at ScienceDirect

Materials Science & Engineering A

journal homepage: www.elsevier.com/locate/msea

On the accumulation of irreversible plastic strain during compression loading of open-pore metallic foams

Alexander Martin Matz[a,b,*], Bettina Stefanie Matz[b], Norbert Jost[b], Gunther Eggeler[a]

[a] Institute for Materials, Ruhr-University Bochum, Universitätsstraße 150, 44780 Bochum, Germany
[b] Institute for Materials and Material Technologies, Pforzheim University of Applied Sciences, Tiefenbronner Straße 65, 75175 Pforzheim, Germany

ARTICLE INFO

Keywords:
Metallic foams
Aluminum
Zinc
Mechanical properties

ABSTRACT

The accumulation of plastic strain as an essential element of the compression behavior of metal foams is investigated by analyzing effective stress-strain curves which were recorded during testing. By applying loading/unloading cycles within the low-strain region until reaching the stress plateau, it is studied how reversible elastic deformation is gradually transformed into irreversible plastic deformation and it is shown that both, elastic and plastic strains, contribute to the total strain ε. This behavior is found to be independent on the investigated mesostructural foam morphologies. Furthermore, a method is derived which can be used to determine a proof stress $\sigma_{\phi_{\mathrm{Pl}}=0.5}$ at which yielding dominates the deformation of a metal foam.

1. Introduction

Open-pore metal foams represent a new class of advanced engineering materials which outperform other materials due to their unique combination of structural and functional properties [1–3]. Especially their mechanical properties are of interest for various kinds of structural applications. Therefore, many investigations of their behavior during compressive loading have been performed [4–20]. It is common to use effective stresses and strains when describing the mechanical behavior of a metallic foam. The characteristics of the stress-strain response are, however, interpreted in different ways which mainly relates to the region between the onset of deformation and the beginning of a stress plateau. This is the major region of interest when thinking of construction design criterions. In this early stage of deformation, a linear increase of stress σ can be observed as a function of strain ε. Hence, this region has been thought of as being of linear-elastic nature (cf. e. g. [1,4,12,13]). However, in other studies [5,14] it has been interpreted as representing an elastic-plastic deformation. In [15,16], the initial region of the stress-strain curve (before reaching the plateau regime) is divided into a linear-elastic and an adjacent elastic-plastic transition zone. But it is not clear how reversible elastic and how irreversible plastic deformation evolve at low total compressive strains. Based on results from loading/unloading experiments, it has been reported that the slope of the initial loading curve is smaller than at slightly higher strains [6,7,10,11,17,18,20]. Consequently, plasticity seems to already contribute to the overall deformation at very little effective strains ε. In this context, sample preparation prior to testing has been mentioned as a reason for uncertainty: A slight deficit in flatness or parallelism can dominate the early mechanical response [18] as well as in some cases only a single strut which is extruded from the surface [11] since only/mainly the part of the foam specimen which is in direct contact with the compression plates accounts for the initial strain response. Additionally, the structural nature of the foam morphology also needs to be considered. We must keep in mind that the effective foam stress corresponds to a distribution of much higher true stresses acting in the strut assembly of the foam [6,7,10,20,21]. Likewise, small effective foam strains result from distributions of much higher strut deformations which have found to be the main reason for this behavior.

In the present work, we investigate the effective foam stress-strain curves which evolve during compression testing when loading/unloading cycles are imposed. In our compression tests we use displacement controlled compressive loading, applying effective foam loading strain intervals as small as $\varepsilon = 0.001$. On unloading, tests are interrupted when a compressive load of $F = 15\,\mathrm{N}$ is reached. Then the next loading strain interval is applied, followed again by unloading to $F = 15\,\mathrm{N}$. This type of loading and unloading is repeated up to 38 times for each of nine foam morphologies which are investigated in the present study. We interpret the resulting stress-strain response in the light of the underlying deformation and damage processes. Special emphasis is placed on the evolution of the partitioning of the total effective strain into reversible elastic and irreversible plastic components with increasing numbers of compressive loading/unloading cycles. The results contribute to a better understanding of the evolution of plasticity and

* Corresponding author at: Institute for Materials, Ruhr-University Bochum, Universitätsstraße 150, 44780 Bochum, Germany.
E-mail addresses: alexander.matz@ruhr-uni-bochum.de, alexander.matz@hs-pforzheim.de (A.M. Matz).

https://doi.org/10.1016/j.msea.2018.05.012
Received 28 December 2017; Received in revised form 3 May 2018; Accepted 4 May 2018
Available online 05 May 2018
0921-5093/

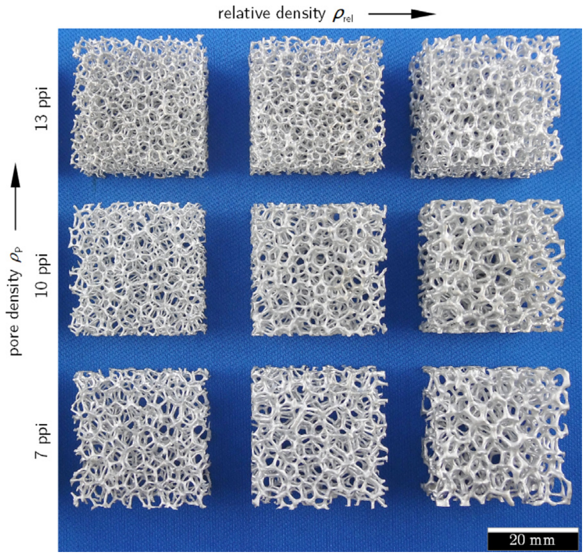

Fig. 1. Investigated foam morphologies (left to right: increasing relative density ρ_{rel}; bottom to top: increasing pore density ρ_P).

damage in metallic foams subjected to compressive loading.

2. Material and methods

Open-pore aluminum foam samples are manufactured using a modified investment casting process as described in detail in [21,22]. Their pore densities

$$\rho_P = \frac{n_P}{l}, \tag{1}$$

with n_P as the number of existing pores on a certain length l, are 7 ppi (pores per inch), 10 ppi and 13 ppi. The relative density

$$\rho_{rel} = \frac{m_{mf}}{m_s} \tag{2}$$

wherein m_{mf} is the mass of the metal foam and m_s is the mass of the solid material, is in the range of 4.94% $\le \rho_{rel} \le$ 11.46%. The investigated foam morphologies are shown in Fig. 1. Detailed information on the mesostructural foam morphologies of the samples investigated is provided in Table 1. The mesostructural parameters are determined by a software-assisted digital microscope of the type VHX-500FD from Keyence NV/SA in Mechelen, Belgium using the measuring techniques described in [21,23].

The alloy used for manufacturing the open-pore metal foam samples

Table 1
Mesostructural parameters of investigated foam morphologies.

Pore density ρ_P (ppi)[a]	Relative density ρ_{rel}	Mean strut length l_{st} (mm)	Mean strut width s_{st} (mm)	Mean pore diameter d_p (mm)	Mean cell diameter d_c (mm)
7	$4.94\%^{+0.56\%}_{-0.64\%}$	2.21	0.53	2.64	5.80
7	$7.44\%^{+0.76\%}_{-0.54\%}$	2.22	0.66	2.44	5.45
7	$10.76\%^{+1.14\%}_{-0.85\%}$	2.19	0.84	2.31	5.22
10	$5.29\%^{+0.39\%}_{-0.52\%}$	2.01	0.52	2.14	5.01
10	$8.04\%^{+1.21\%}_{-0.85\%}$	2.01	0.68	1.96	4.84
10	$11.46\%^{+1.36\%}_{-1.22\%}$	2.02	0.84	1.82	4.59
13	$6.57\%^{+0.51\%}_{-0.79\%}$	1.55	0.44	1.61	3.83
13	$8.46\%^{+0.70\%}_{-0.81\%}$	1.55	0.60	1.52	3.61
13	$11.09\%^{+0.82\%}_{-0.50\%}$	1.56	0.78	1.42	3.38

[a] Nominal values provided by the manufacturer.

Table 2
Chemical composition of the starting material.

Alloy	Si	Fe	Cu	Mg	Zn	Al
Al-11Zn	0.0038%	0.0097%	0.0085%	0.0016%	10.865%	Bal.

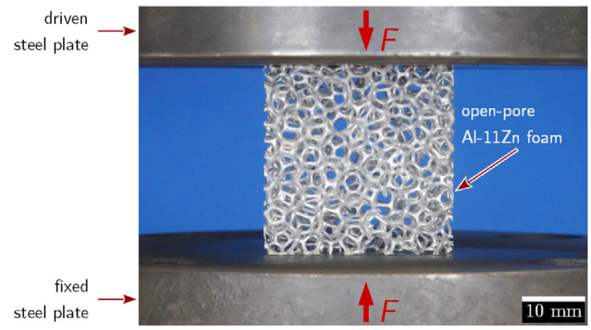

Fig. 2. Experimental set-up for compression tests of open-pore Al-11Zn foams.

is Al-11Zn (wt%) containing less than 0.01% of other elements. The composition is analyzed by spark emission spectroscopy that is shown in Table 2. Electrical discharge machining [24] is applied to achieve specimen dimensions of $30 \cdot 30 \cdot 20\,mm^3$. The as-machined samples are homogenized at a temperature of $\vartheta = 400\,°C$ for $t = 2\,h$ and then quenched in water. Subsequently, the samples are cold-aged at room temperature for $t > 100\,h$ to achieve finely dispersed GP-Zones [25].

Compression tests are performed using a TesT universal test rig P112.20kN.H. Compressive forces are applied on the samples by hardened precision-grinded steel plates (cf. Fig. 2). Prior to testing, these are treated with a graphite lubricant to keep friction effects at a minimum. Before testing the samples, these plates are carefully aligned by way of end-gauge calibrations. A displacement rate of 0.9 mm/min is applied which corresponds to an initial strain rate of $5 \cdot 10^{-4}\,s^{-1}$. Load-displacement data were recorded to obtain the effective stress-strain histories. The sampling rate was $f = 4\,s^{-1}$. All tests were interrupted and discontinued at a displacement of $s = 24\,mm$ which corresponds to a maximum effective strain of $\varepsilon = 0.8$. In intervals of $\Delta s = 0.03\,mm$ in the range of $0 < s \le 1.14\,mm$, loading/unloading intervals were performed to gain information on the accumulation of irreversible plastic strain within the region between the onset of deformation and the beginning of the plateau regime. Eight loading/unloading steps are performed within the plateau regime and densification regime at certain strains ε. On unloading, tests are suspended when a compressive load of $F = 15\,N$ is reached. Then, the next loading strain interval is applied followed by unloading to $F = 15\,N$. In this study, loading/unloading intervals in the range of $0 < \varepsilon \le 0.03$ are considered.

For comparison purposes, bulk compression test specimens were fabricated out of continuous cast primary material in dimensions of $d_0 = 4\,mm$ in diameter and $h_0 = 6.5\,mm$ in height. They were tested according to DIN EN ISO 50106 using the universal test rig mentioned above.

3. Results

A typical stress-strain curve on the example of an Al-11Zn foam with a pore density of ρ_P = 7 ppi and a relative density of ρ_{rel} = 5.16% is shown in Fig. 3(a). The region of onset in deformation until reaching plastic collapse is present within a strain range of $0 \le \varepsilon \le 0.0284$. An amplification of this region is presented in Fig. 3(b), showing the first 38 loading/unloading intervals. As a typical response of elastic-plastic foams, at a first glance, a linear increase in strength σ as a function of strain ε can be observed which diminishes in strength until reaching a local maximum associated with plastic collapse (corresponding to the